COMPARISON OF LABORATORY MEASURED RESISTIVITY INDEX AND CAPILLARY PRESSURE WITH IMAGED BASED CALCULATIONS AND NETWORK MODELLING PREDICTIONS

S. Yanici[1], Y. Cinar[1], C.H. Arns[1], J. Y. Arns[1], W.V. Pinczewski[1], M.A. Knackstedt[2], M. Touati[3], V.S. Suicmez[3]

(1) School of Petroleum Engineering, University of New South Wales, Sydney, Australia
(2) Applied Maths, RSPhysSE, Australian National University, Canberra, Australia
(3) Saudi Aramco Oil Company, Dhahran, Saudi Arabia

This paper was prepared for presentation at the International Symposium of the Society of Core Analysts held in Noordwijk aan Zee, Netherlands, 27-30 September, 2009.

ABSTRACT

This paper presents comparisons for resistivity index and capillary pressure between laboratory measurements on conventional core plugs and predictions of the image-based techniques and network modelling.

The laboratory measurements were carried out using a combined, 4-electrode Pc/RI apparatus based on the porous plate technique. A simple 2wt% NaCl brine-air system was used in the experiments. The porous systems investigated include a carbonate core from a Middle Eastern reservoir, an outcrop limestone (Mt Gambier) and outcrop sandstone (Fontainebleau). The predictions of porosity, permeability, formation factor, capillary pressure and resistivity index were made using the image-based techniques and network models. The validity of the predictions was then compared with the laboratory data.

The comparisons show that both predictive tools have a good agreement with the laboratory data for porosity and formation factor while overestimate the laboratory permeability. The results demonstrate that, above a water saturation of 30%, both laboratory measurements and predictions follow the Archie behaviour. Below 30%, however, a "non-Archie" behavior is generally observed. The image based calculations and laboratory measurements are generally close to each other for the outcrop samples whereas the network model shows slightly different results for the reservoir carbonate. The pore entry radii calculated using the image-based technique and network models show similar results only for the outcrop sandstone. The reasons for the poor estimations are assumed to be due to poor image quality or insufficient resolution for feature imaging and sample size or scale dependence.

INTRODUCTION

Resistivity index and capillary pressure are two key elements among others in estimating hydrocarbon reserves. Porous plate technique is one of the methods used commonly to obtain both petrophysical properties simultaneously, although this technique consumes long time and requires costly special core handling.

A quick and cost effective approach is utilizing micro-CT imaging technique. It is now possible to use micro-CT imaging of small, irregularly shaped rock samples (rock

fragments, sidewall cores and unconsolidated rock samples) to predict both capillary pressure and resistivity index either directly from the images or from network models based on the micro-CT images. Although further work is needed to demonstrate that micro-CT based predictions are comparable to laboratory measurements on conventional core plugs, this emerging technology has the potential to overcome the time and cost limitations associated with conventional and special core analysis methods.

The computation of electrical properties and capillary pressure directly from micro-CT images is a recent technique. Knackstedt *et al.* (2007) have calculated the electrical resistivity index of a carbonate rock directly from images using a fast conjugate-gradient method. A comparison of calculations has been presented with the laboratory results obtained using the sister plugs (Padhy *et al.* 2005, 2006). Values of the computed saturation exponent on the carbonate sample were slightly smaller than that obtained from experiments. This difference has been attributed to natural heterogeneity and perhaps the use of a similar but not the same sample.

Resistivity index and capillary pressure can also be predicted by network modelling which is based on micro-CT images. Arns *et al.* (2007) have recently compared the image based calculation methods and the network models that use networks constructed from the micro-CT images. Three samples, consolidated sandstone, unconsolidated sandstone and a carbonate sample were used to match the permeability and wetting fluid distribution of the rock. Permeability was in good agreement when the large images used. Recently, Youssef *et al.* (2008) have analysed the petrophysical properties (F and RI-Sw) of carbonate samples which were measured in the laboratory and predicted using the micro-CT based network modelling. They have concluded that the image based network modelling and experimental results match perfectly for homogeneous samples. However, for bimodal sample, good agreement between experimental and computational results depends on the conductivity length of microporosity.

Recently, Han *et al.* (2009) have studied the non-Archie behaviour. They used a centrifuge technique to obtain the electrical response for the clay-free Fontainebleau sandstone. They simulated the results using the quasistatic capillary displacement and minimization of the interfacial energy to distribute wetting phase in the 3D pore space. Moreover, Kumar *et al.* (2009) have applied an image registration technique which allows visualizing multiple fluid distributions within the core to understand the effect of wettability on electrical properties of the rock. They have reported a good match between the experimental and numerical results of the resistivity response.

This paper presents a comparison between laboratory measurements of the resistivity index and capillary pressure and micro-CT based computations. Sister plugs of 125 mm^3 from Fontainebleau, Mt Gambier and a carbonate reservoir were used to obtain micro tomographic images. Core samples of larger than 12,870 mm^3 were used in the laboratory measurements.

ROCK TYPES

Three rock types were used in this paper. The first sample is Fontainebleau Sandstone, which is clay free quartz and well sorted homogenous sandstone. The second sample is a highly porous and permeable quarried fossiliferous outcrop limestone from Mt.

Gambier, Australia. It has zero microporosity. The last sample is a carbonate rock from Middle East. **Fig-1** shows small subsets of micro-CT images of the three samples.

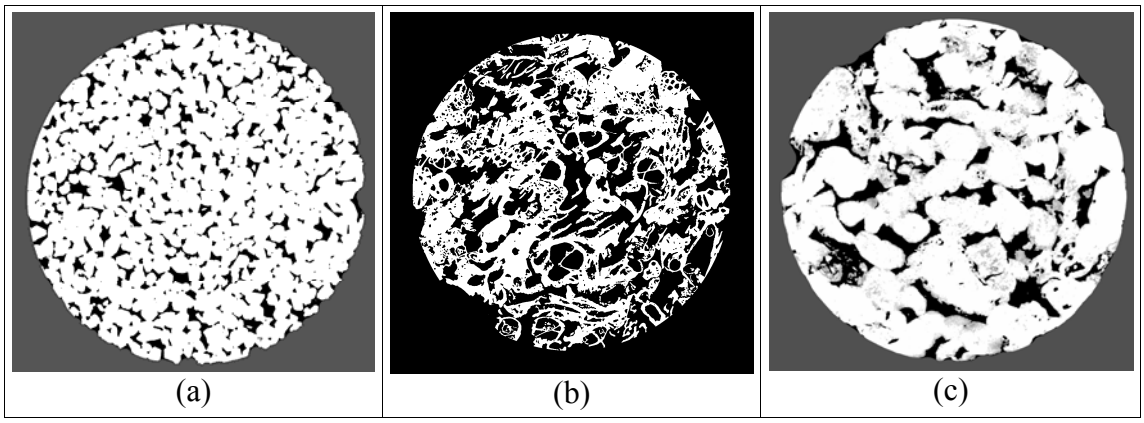

Fig-1: Micro-CT images of (a) Fontainebleau (b) Mt. Gambier and (c) Middle Eastern Carbonate.

Table 1 gives a summary of the laboratory measured and image-based and network modeling predicted petrophysical properties of all three samples. The data shows that the porosity and formation factor measurements from the laboratory agree well with the calculated results. However, we have obtained a clear overestimation of the laboratory measured permeability from the image-based and network modeling. It is premature to make definitive conclusions regarding the applicability of the method to estimate permeability. However, the reasons for poor estimation could come down to a number of possible factors such as poor image quality or insufficient resolution for feature imaging and sample size/scale dependence. A detailed discussion on the potential reasons is well documented in Touati *et al.* (2009).

Table 1. Measured and predicted petrophysical properties of the samples.

		Fontainebleau	**Mt.Gambier**	**Middle Eastern Carbonate**
Image Size			960^3	800^3
Voxel Size (µm)				
Porosity (%)	Experiment	16.0	51.7	20.2
	Image	16.0	43.9	23.2
	Network	20.0	40	20.5
Permeability(D)	Experiment	n/a	4.1	0.5
	Image	1.3	9.6	5.1
	Network	1.5	12.2	7.6
Formation Factor	Experiment	25.8	7.3	21.2
	Image	30. 7	8.3	17.1
	Network	25.8	7.3	16.9

METHODOLOGY

Core Preparation
Before the porous plate experiment, the dry weight and dimensions of each core were measured. The core sample was then evacuated for 12 hours and saturated using a 2% by weight NaCl brine. The diameter of the core sample was 1 inch for Fontainebleau and Mt. Gambier samples and 1.5 inch for the Middle Eastern carbonate. A small plug with 5mm in diameter was drilled from the top of each core sample and used for the micro CT X-ray scans. Therefore, we note here that comparisons between the core analysis measurements and predictions made may represent different heterogeneities. This needs especially to be considered for the carbonate sample. Olafuyi *et al.* (2006) have reported a negligible effect of the core-to-pore scaling on the capillary pressures for homogenous outcrop sandstones.

Porous Plate Technique
In this technique, a fully brine saturated core sample is displaced with air under constant capillary pressure by means of a semi-permeable porous plate that does not allow the non-wetting phase to flow through. In each constant capillary pressure, brine production from the desaturating core and electrical resistance are observed as a function of time until no change in both data is recorded. The capillary pressure is then increased into a new value and the above defined observation is continued. This process continues until irreducible brine saturation is reached where there is practically no brine production. For the cases where the core samples have low permeability, irreducible brine saturation cannot be obtained due to the limitation on the threshold pressure of the porous plate, which is 10 bars for brine-air system in this study. The saturations are determined from the brine production data. When the experiment is ceased, the weight of the core sample is measured to validate the brine saturations.

The Pc/RI experimental apparatus developed and built by Ergotech Ltd. Pty. (UK) was used in the experiments. The volumes of the brine produced during the experiments were collected in the burettes of an accuracy of 0.1 ml. The digital pressure transducers of Drug Co. with 0.01 psi (0.07kPa) were used to measure capillary pressure. The Agilent 4263B LCR meter was used to measure resistance with ±0.001 ohm accuracy. Two methods have been reported in the literature for the measurement of resistance; ‘two-electrode method’ and ‘four-electrode method’. Moss *et al.* (2000) observed that the two electrode method causes polarization at the rock-electrode contact for the frequency range of 10Hz-10kHz. Bona *et al.* (2008) have also studied the effect of frequency range on both methods. They have concluded that the two-electrode method gives more reliable results at a high frequency range (>1 kHz) while the four-electrode method is more adequate for the low frequency range (0.1-1 kHz). Hence, we carried out the resistivity index measurements at 1 kHz using the four-electrode method. A sketch of the method applied to measure the combined capillary pressure and resistivity index is depicted in **Fig-2**.

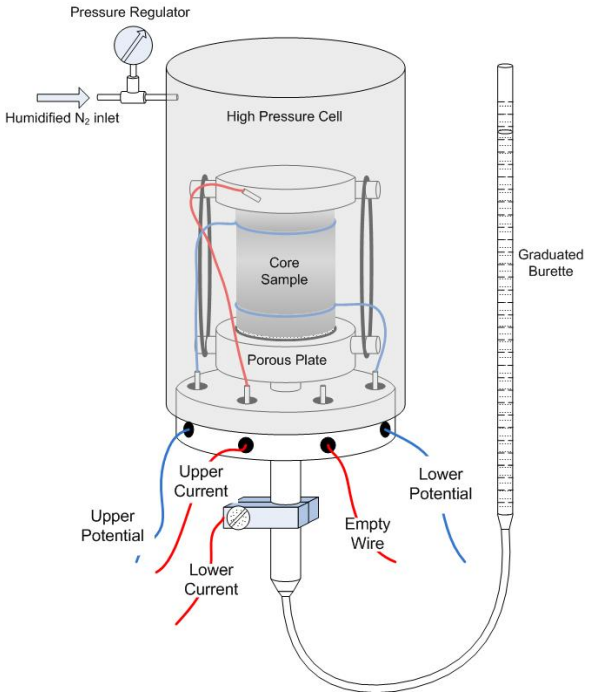

Fig-2: The porous plate technique for resistivity index and capillary pressure measurement.

Acquisition of 3D X–Ray CT Images

Conventional medical CT provides not only millimetrical resolution for meter to decimeter scale objects, but also supplies the data which is useful for the measurement of density. However, these instruments are insufficient to examine the pore scale structure. Therefore, a high resolution and large field X-ray μ-CT facility has been constructed to analyze the 3D structure of the rocks.

A 3D representation of a structure is formed commonly known as tomogram which is a data set generated by a Tomography. X-rays are used to probe the specimen. An X-ray camera records the series of radiographs at different viewing angles by rotating specimen to generate a tomogram. This set of radiographs, projection data, is processed with a reconstruction algorithm.

The X-ray source and detector (scintillator CCD) are located at an optimum distance to acquire high resolution and maximal field of view (FOV) as shown in **Fig-3.** Pixels of 2048^2 at a depth of 16 bits per pixel can be recorded by the X-ray camera. The specimen rotation stage has an angular accuracy of 0.001°. Magnifications can be adjusted between X1.1 to over X100 by changing the position of the X-ray camera and rotation stage. The large range of X-ray energies helps to identify the contrast between the different phases such as water and oil in reservoir core plugs. Moreover, fine features can be discriminated from the dense materials by the large dynamic range of the X-ray camera. Filters are used to reduce beam hardening artifacts which are caused by polychromatic X-rays in the tomogram.

The camera is placed to the maximum possible distance to reduce reconstruction artifacts associated with cone beam tomography. Youssef *et al.* (2008) have mentioned that increasing the pixel size reduces the noise and enhances image contrast. However, this causes to increase image acquisition time. It takes approximately 40 hours to

generate 2048^3 voxel tomograms. The number of radiographs in a tomographic series is roughly around 1.5 times the number of pixels across the radiograph. The Feldkamp technique is used to reconstruct the tomographic series (Feldkamp *et al.*, 1984).

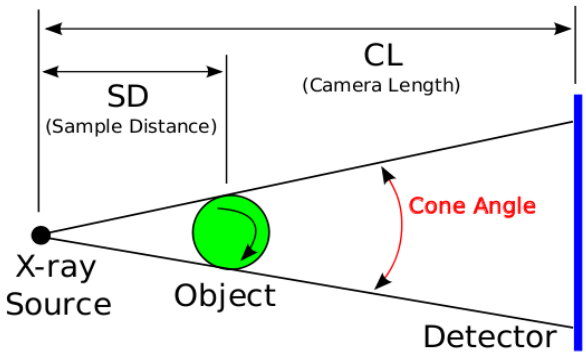

Fig-3 Experimental X-ray CT apparatus.

Phase Identification

Each voxel has an X-ray attenuation coefficient value which allows separating the phase system into the pore and mineral phases. This identification of the system is easily made for the clean sandstone because of the simple bimodal attenuation distribution. However, it is very difficult to distinguish between the microporous and solid mineral phases for the carbonates. Each voxel should be well-defined and labeled to analyze tomograms successfully.

Selecting single threshold attenuation according to the bulk measurement of porosity on the original core is the easiest way for phase identification. Undesirably, heterogeneity of the rock and amount of peak overlap in the intensity histogram cause lack of success in this method. Besides, micropores increase the uncertainty of single threshold technique. Another technique, an edge based kriging segmentation algorithm introduces two cutoff attenuation coefficients to distinguish between pore and rock regions. Lower cutoff is an upper limit for the pores and higher cutoff is a lower limit for the grain phase. The unknown region between these phases can be identified with the kriging indicator. Porosity would be lower than conventional porosity measurement because of poor image resolution.

Computational Methods

Resistivity Index

Electrical conductivity is measured directly from Micro-CT image data by using finite element method (Garboczi & Day, 1995; Arns, 2002) which uses a variational formulation of the linear conductivity and solves the Laplace equation by minimizing a fast conjugate-gradient method. Along the each direction of the tomogram, formed approximately 1000 voxels, voltage gradients are applied to calculate conductivity. Each voxel is taken to be trilinear finite element. Boundary conditions are assumed to be non-periodic. Water conductivity is 1, oil and solid conductivities are assumed zero to calculate resistivity. The resistivity calculation is based on extremely wetting condition such as strongly oil-wet or strongly water-wet because wettability affects the

fluid distribution within the pore. For example, in the water-wet rocks, brine prefers to locate in the small pores and to make film on the rock surface. However, oil moves to bigger pores and brine surrounds oil blocks. When the brine is displaced with oil, brine connection can still remain because of the brine film.

For the drainage process, pore spaces in the image are assumed to be filled fully with water. The largest pore is displaced first with the non-wetting phase and the wetting phase saturation is calculated after the non wetting phase invasion. This stepwise procedure is continued until irreducible water saturation is reached. For the imbibition experiment, the thickness of the wetting film is increased in the small pores. Man and Jing (2002) studied in more details for different wetting scenarios and displacement processes.

Drainage Capillary Pressure

Pore and grain phases are separated in each point of voxelated images and the largest diameter of the sphere is defined as covering all pore phases. One assumption to be made is that all spheres radii are greater than or equal to the equivalent pore entry radius. Measurement of capillary pressure and non-wetting phase saturation starts with the largest sphere because capillary pressure is very low in the large pores. While the diameter of the pore is decreasing and capillary pressure is increasing stepwise, non-wetting phase flows through the pore space and displacing the wetting phase. The wetting phase saturation decreases as the displacement process continues. The saturation of the non-wetting phase is calculated by dividing the total volume of the invaded sphere to the total volume of pore space. A boundary condition is applied to make a comparison with the laboratory measurement of capillary pressure and wetting saturation. For this reason, the wetting phase is displaced only from one side of the core like a similar condition prevailed in the laboratory measurements.

Network Representation: Methodology and Ambiguities

The construction of a network representation of pore space from the image starts with partitioning the porous space. An Euclidean distance map is calculated after the pore and grain phases are separated from the disconnected components and this map is covered with the radius map to identify a potential pore centre (Sheppard *et al.,* 2006). Then, centres are used as seed points for a watershed partitioning (Russ 2007). Finally, pore-bodies are merged if the junction is sufficiently wide to be judged. With this final step, the number of pores merging can be identified. Finally, 3D network images are constructed as seen in **Fig-4**. Sheppard *et al.* (2006) have concluded that the partition of subvolume has still unwanted uncertainties. To illustrate this, a single pore or two distinct pores may be separated by a throat. However, Arns *et al.* (2007) have mentioned that, although pore merging causes different networks which have different numbers of pores, pore and throat sizes and coordination numbers, this network transport properties show reasonable results with one of the imaged rock.

Resistivity index is significantly affected by the wetting phase continuity. To understand the wetting phase continuity, Arns *et al*. (2007) have used pore partitioning and algorithm where pore has at least two connections from the neighbour pores with the wetting phase. The coordination number is also very useful parameter to understand the wetting phase continuity. Some throats at the wetting phase connection disappear at the low wetting saturation because of the reduction in the coordination number.

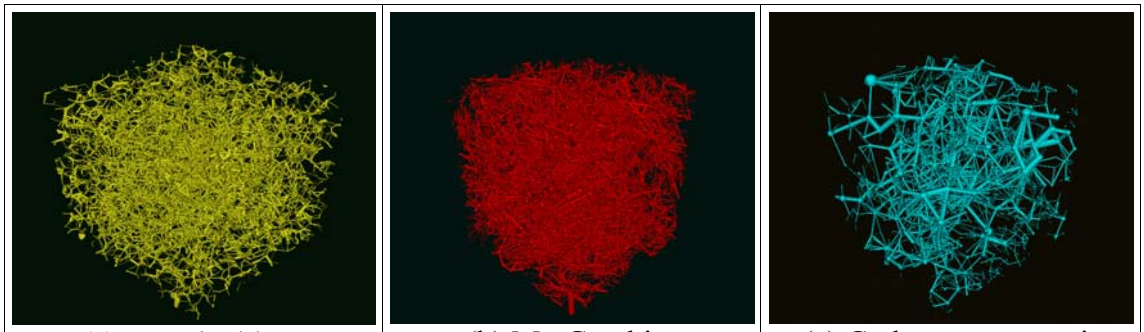

(a) Fontainebleau (b) Mt. Gambier (c) Carbonate reservoir

Fig-4: 3-D Network images of the samples.

RESULTS

Fontainebleau

Fig-5 shows comparisons between measurements and predictions of resistivity index and capillary pressure for the Fontainebleau sandstone. For the water saturations of 1 to 0.5, the laboratory data as well as the image-based and network model predictions agree very well with the Archie behaviour. Below that point, both predictions show very different results; the image-based method yields a bending up non-Archie behaviour whereas the network model indicates a bending down non-Archie behaviour. The laboratory observation of resistivity index shows a non-Archie behaviour similarly to the network model output, but it deviates from the Archie behaviour at a bit lower saturation, i.e. 30%. It is, however, to note that it is widely accepted that clay-free clean sandstones like Fontainebleau sandstone should follow an Archie behaviour. One can argue that the measurements under ambient and reservoir conditions might have caused these different observations. The laboratory data presented here, on the other hand, agrees well with the data reported by Durand (2003) and Han *et al.* (2009). Both predictive tools, however, match the laboratory data for capillary pressure with great success as shown in **Fig-5b.**

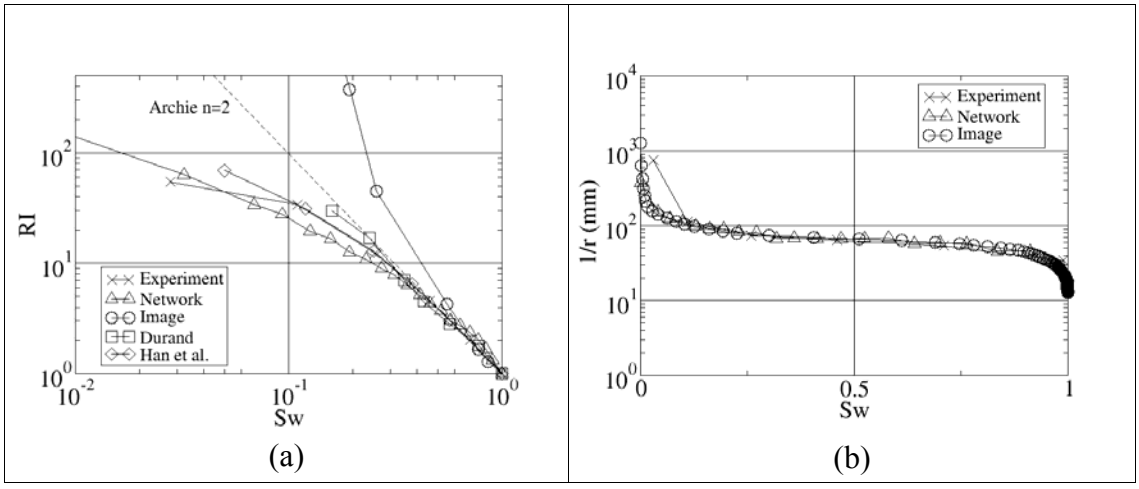

Fig-5: Comparison of (a) resistivity index and (b) capillary entry radius for the Fontainebleau sample.

Mt. Gambier

The results with the quartz-rich carbonate Mt. Gambier show a different behaviour of resistivity index from which observed with the Fontainebleau sandstone (**Fig-6a**). The image-based prediction and the laboratory data have close results, perfect Archie behaviour especially for the saturations above 30%. But for the saturations below 30%, the image-based predictions bend up slightly, showing a complete opposite behaviour the laboratory data shows. The laboratory data shows a slight bending down. The resistivity index predicted by the network model follows an Archie-type straight line with an exponent higher than 2. **Fig-6b** shows a perfect match between both predictions for capillary pressure, but a distinct difference between them and the experimental observation.

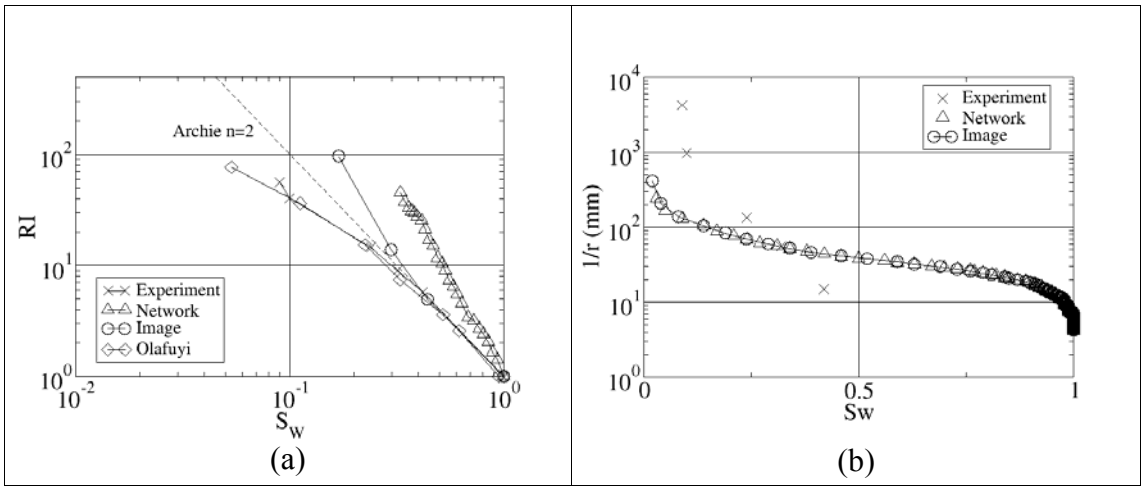

Fig-6: Comparison of (a) resistivity index and (b) capillary entry radius for the Mt. Gambier sample.

Middle Eastern Carbonate Reservoir

Fig-7a shows that the resistivity index of the reservoir core is predicted well using the image-based technique. The network model yields approximately two different straight lines with a high exponent for the high water saturations and a low exponent for the low saturations. The threshold saturation for both straight lines is nearly 20%. **Fig-7b** shows the pore entry radius versus water saturation results. Again, both prediction models yield almost the same results while differing from the laboratory data significantly. The reason can be the effect of pore space roughness. At the low water saturations, microporosity effect is observed on laboratory measurement and image based calculation.

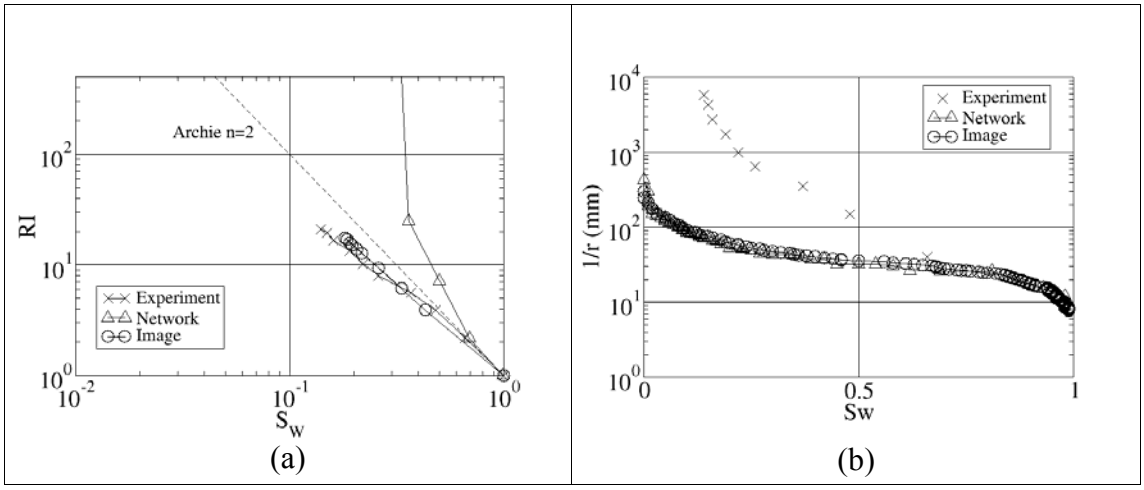

Fig-7: Comparison of (a) resistivity index and (b) capillary entry radius for the Middle Eastern carbonate reservoir sample.

DISCUSSION

For the homogeneous Fontainebleau sample, capillary pressure results match well for all methods. Only, resistivity index results of network model show different trends at low water saturations. This can be explained by the continuity of the wetting film because of surface roughness.

The results of the electrical properties of Mt. Gambier show similar agreement with the image-based prediction and the experimental observation. The network model gives quite a bit different results, which can be explained by the shape factor. The capillary pressure calculations using the image-based and network model shows similar behaviour. Experimental results are quite different from the calculations. The reasons for this can be the size and boundary effects.

Network model predictions bend up at low water saturations. The shape factor and continuity of the wetting film can be arguably considered as the reasons. The calculated microporosity of the reservoir carbonate is approximately 17.5% of the total porosity (3.6%+16.9%=20.5%). This amount may be relatively small for a large effect on the petrophysical properties. The image- and network-based calculations of capillary pressure do not match well with the laboratory results. The different sample size, sister plug and boundary effect can be the main reasons for the mismatch.

CONCLUSIONS

The porous plate laboratory experiments as well as the micro-CT image-based and network model predictions of capillary pressure and resistivity index on three different porous samples (Fontainebleau sandstone, Mt. Gambier carbonate and a carbonate reservoir) were presented. Comparisons between the laboratory data and predictions were reported.

From the comparisons, it was concluded that, generally, the resistivity index can be predicted using both predictive tools with some success for the water saturations above nearly 30%. The resistivity indexes of this high saturation region mostly follow the Archie behaviour. However, the comparisons for the water saturations below 30%

indicate that the prediction of resistivity index success is rather poor. It seems that the prediction capability depends on the rock type.

The experimental observation of the capillary pressure of the sandstone is predicted well with both predictive tools. However, although both predictive methods yield almost the same results, they differ significantly from the porous plate experimental data for both carbonate core samples.

ACKNOWLEDGEMENTS

The authors acknowledge the member companies of the Digital Core Consortium for their support. We thank Saudi Aramco Oil Company for permission to present some of the data in this work. We thank the A.N.U. Supercomputing Facility and the Australian Partnership for Advanced Computing for very generous allocations of computer time. This work is supported by the Australian Research Council through the Discovery Grant DP0878564.

REFERENCES

1. *C. H. Arns, M. A. Knackstedt, W. V. Pinczewski, and E. J. Garboczi: 2002, "Computation of linear elastic properties from microtomographic images: Methodology and agreement between theory and experiment" Geophysics, 67:1396-1405.*

2. *M.A. Knackstedt, C.H. Arns, A. Limaye, A. Sakellariou, T.J. Senden, A.P. Sheppard, R.M. Sok, W.V. Pincewski, and G.F. Bunn: 2004, "Digital Core Laboratory: Properties of reservoir core derived from 3D images", SPE87009.*

3. *C.H. Arns, F. Bauget, A. Limaye, A. Sakellariou, T.J. Senden, A.P. Sheppard, R.M. Sok, W.V. Pinczewski, S. Bakke, L.I. Berge, P.E. Øren and M.A. Knackstedt: 2005, "Pore-Scale Characterization of Carbonates Using X-Ray Microtomography", SPE90368.*

4. *Olafuyi, A.O., Sheppard, A.P., Arns, C. H., Sok, R.M., Cinar, Y., Knackstedt, M.A. and Pinczewski, W. V.: 2006, "Experimental Investigation of Drainage Capillary Pressure Computed from Digitized Tomographic Images" Society of Petroleum Engineers, SPE 99897, In Proceedings of the SPE/DOE Improved Oil Recovery Symposium, Tulsa, OK, April 22-26.*

5. *M. A. Knackstedt, C. H. Arns, A. P. Sheppard, T. J. Senden, R. M. Sok, Y. Cinar, A. O. Olafuyi, W. V. Pinczewski, G. Padhy, and M. Ioannidis: 2007, "Pore Scale Analysis of Electrical Resistivity in Complex Core Material", International Symposium of the Society of Core Analysts - SCA2007-33, Calgary, Canada.*

6. *N. Bona, E. Rossi, S. Capaccioli, M. Lucchesi and Largo Bruno Pontecorvo: 2008, "Electrical Measurements: Considerations on the Performance of 2- and 4-Contact Systems", International Symposium of the Society of Core Analysts - SCA2008-07, Abu Dhabi, UAE.*

7. *Garboczi, E. J. and Day, A. R.: 1995, "An algorithm for computing the effective linear elastic properties of heterogeneous materials: 3D results for composites with equal phase Poisson ratios", J. Mech. Phys. Solids, 43(9), 1349-1362.*

8. *S. Youssef, D. Baued, M. Han, S. Bekri, E. Rosenberg, M. Fleury, and O. Vizika: 2008, "Pore-Network Models Combined to High Resolution μ-CT to Asses Petrophysical Properties of Homogeneous and Heterogeneous Rocks", IPTC 12884.*

9. *H.N. Man and X. D. Jing: 2002, "Network modeling of mixed wettability on electrical resistivity, capillary pressure and wettability indices", Journal of Petroleum Science and Engineering, 33, 101-122.*

10. *M. Han, S. Youssef, E. Rosenberg, M. Fleury and P. Levitz: 2009, "Deviation from Archie's law in partially saturated porous media: Wetting film versus disconnectedness of the conducting phase", Physical Review E, 79.*

11. *M. Kumar, M. A. Knackstedt, T. J. Senden, A. P. Sheppard, C. Arns, S. Yanici and Y. Cinar: 2009, "Mapping fluid distributions in 3D at the pore scale: Quantifying in the influence of wettability and saturation history on rock resistivity", SCA2009.*

12. *C. Durand: 2003, "Improvement of fluid distribution description during floods by combined use of X-ray CT-scan and continuous local resistivity measurements", SCA2003-29.*

13. *L. A. Feldkamp, L. C. Davis and J. W. Kress: (1984), "Practical cone-beam algorithm", Journal of Optical Society of America, 1(6), 612-619.*

14. *M. Touati, S. Suicmez, J. Funk, Y. Cinar, M. Knackstedt: (2009), "Pore network modeling of Saudi Aramco rocks: A comparative study", SPE Saudi Arabia Section Tech Symp and Exhib, AlKhobar, 9-11 May.*

15. *A. K. Moss, X. D. Jing and J. S. Archer: (2000), "Wettability of reservoir rock and fluid systems from complex resistivity measurements", International Symposium on Evaluation of Reservoir Wettability and Its effect on Oil Recovery, New Mexico, USA.*

16. *O. O. Adisa: (2008), "Experimental investigation of Two-Phase flow porperties of core samples from conventional core to micro-CT imaging scales", PHD Thesis, UNSW, Australia.*